Available online at www.sciencedirect.com

ScienceDirect

Procedia Engineering 86 (2014) 184 – 194

Procedia Engineering

www.elsevier.com/locate/procedia

1st International Conference on Structural Integrity, ICONS-2014

Dissimilar Electron Beam Welding of Nickel base Alloy 625 and 9% Cr Steel

C. Wiednig[a,*], C. Lochbichler[b], N. Enzinger[a], C. Beal[a] and C. Sommitsch[a]

[a]*Institute for Materials Science and Welding, Graz University of Technology, Austria*
[b]*voestalpine Gießerei Traisen, Austria*
[*]*E-mail ID: christopher.wiednig@tugraz.at*

Abstract

To improve the thermal efficiency of fossil running power plants increasing the live steam temperature is essential. In power plant construction, 9-12% chromium martensitic steels are widely used but if steam temperatures rise above 625°C there is no way around nickel base alloys.

The scope of this study was to ascertain the weldability of cast nickel base alloy 625 with cast martensitic 9% chromium steel COST CB2, using electron beam welding (EBW). Similar (A625/A625) and dissimilar joint welding experiments on 50mm thick plates were executed. Microstructure of welded joints was investigated and mechanical-technological tests were carried out.
Results show that work pieces were completely welded and the microstructure of the seam shows no problems except some δ-ferrite grains near the fusion line on the CB2 side. The joints exhibit good mechanical properties in spite of the presence of a thin layer with very high hardness in the heat affected zone (HAZ) on the CB2 steel side. [1].

Peer-review under responsibility of the Indira Gandhi Centre for Atomic Research

Keywords: Electron Beam Welding; Dissimilar welding; Nickel base alloy; 9% Cr steel;

1. Introduction

The annually growing worldwide energy demand in combination with the prognosticated usage of fossil energy resources will lead to a global increasing of greenhouse gas emission. Improving the thermal efficiency of fossil running power plants is a necessary step to counteract this issue.

Peer-review under responsibility of the Indira Gandhi Centre for Atomic Research
doi:10.1016/j.proeng.2014.11.027

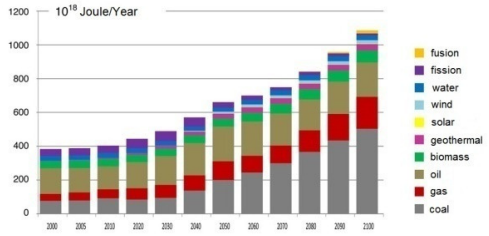

Figure 1: Annual global primary energy demand without CO2 restriction [2]

To achieve this, an increase of the live steam temperature is needed which is a huge challenge for the used materials. Martensitic 9-12% chromium steels are currently the most important materials used in steam and gas turbine technology. They offer an excellent combination of hardness and toughness. Furthermore a high thermal conductivity and a small thermal expansion is present [3]. However, if steam temperatures rise above 625°C there is no way around nickel based alloys. Nickel based super alloys offer superior corrosion behavior and outstanding creep resistance but due to their high price, a well-considered use is indispensable [4], [5], [6]. Engineers, now have to face the problems of combining this material with the 9-12% chromium martensitic steels to apply the best solution at a proper cost level.

This study is a continuation of the diploma thesis written by B. Berger [7], where joining between these two materials by manual arc welding with rod electrodes (MMAW) and gas metal arc welding (GMAW) was investigated. Compared to this process, EBW offer several advantages: single layer (see Figure 2) weld, no filler material, smaller fusion zone, less machining time for joint preparation, less welding time and a fully automated process.

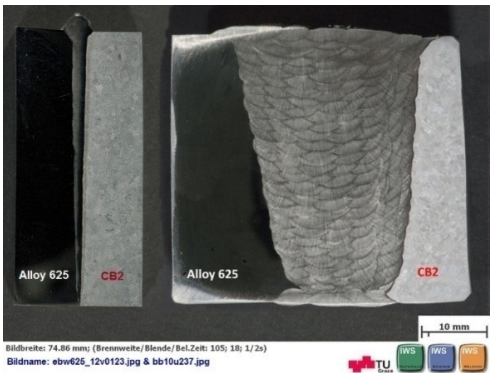

Figure 2: Comparison EBW & MMAW

Electron beam welding is a high quality fusion welding process with a very high energy density (up to 10^9W/cm² [8]). The heating source in EBW is the kinetic energy of electrons. When the electrons hit the surface, they are decelerated in the lattice and transfer their energy to the work piece. At a beam power density above 10^5 W/cm² the deep welding effect occurs. The material evaporates instantly while a steam capillary (keyhole) is created, enabling thick section welding in a single layer.

A very unique characteristic of electron beam welding is its possibility to weld thick walled parts with a single layer. With modern equipment welds up to 200mm in steel are possible [9], [10]. By reason of this special characteristic a very low heat quantity is brought into the work piece [11]. Figure 3 show the temperature measured by two thermocouples (TC) located next to a 50mm thick weld. The temperature 15mm away from the seam centre did not exceed 250°C and also the temperature measured closer to the fusion centre (TC 1) dropped under this

temperature about 60 seconds after the heat source passed this location. This circumstances offers especially in dissimilar welding great advantages [12], [13], [14].

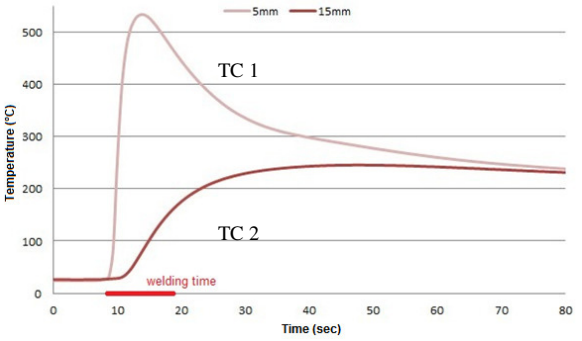

Figure 3: Temperature measurement during EBW

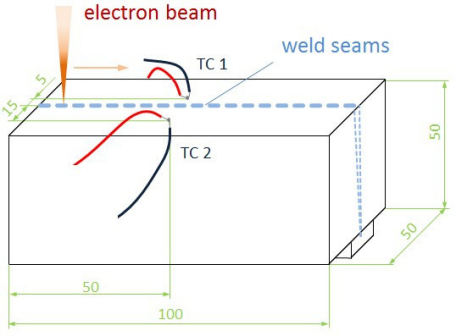

Figure 4: TC Experimental setup

The joining of dissimilar metals is far more complex than producing a similar joint. The difficulties when joining dissimilar materials include the problems when joining each base metal individually, and the problems that occur with their compositions. EBW offers strategies to reduce or overcome these problems to a certain extent [12], [13], [14]:

- The high-energy density can solve the problem of the large difference in melting temperature;
- The thermal conductivity problem can be overcome by directing the beam correctly to the required location;
- The small weld bead size of EB welds minimizes the mixing of dissimilar metals; that limits the brittle zones arising from the chemical mismatch;
- Due to the very small time slot of diffusion permitting temperatures, the intermetallic phase can be kept very small;
- Because of the high temperature gradients and associated rapid solidification of the materials, the solubility limit of elements is shifted to higher concentrations.

2. Experimental Procedure

2.1 Materials

COST CB2: Steels based on 9 - 12% chromium are transformation hardened steels, which are tempered for service. A high density of dislocation and internal interfaces results from the martensitic transformation during cooling after the normalising treatment. After casting, the material was austenitised and tempered at 760°C. Figure 5 shows the tempered martensitic structure of the CB2. The prior austenite grain boundaries are still visible and some precipitates (M23C6 and MX) are identified, which are main contributors to the creep strength [3]. The major alloying elements are listed in Table 1 [15]. Martensitic chromium steels are difficult to weld. The high carbon content requires a complicated temperature control including pre heating, defined interpass temperature, cooling and a post weld heat treatment.

A625: The material number of the alloy 625 is 2.4856. The microstructure of the alloy is cubic face-centred and there are no phase transitions in the solid state. A625 is strengthened mainly by carbon, chromium, molybdenum and niobium. The high strength is achieved by solid solution hardening (Mo, Nb) and by precipitation hardening which is mainly derived from the metastable γ‘‘ phase [Ni3(Nb,Al,Ti)]. The huge grain size is conducive to creep resistance. The high amount of pores is typical for cast material (see Figure 6). [5], [6]. The material was delivered in solution annealed condition. The major alloying elements are listed in Table 2 [16]. This nickel based alloy has a good weldability but as all nickel alloys it is extreme prone to hot cracking in presence of sulphur (low melting Ni-Ni3-S2 eutectic) [17].

Figure 5: COST CB2 microstructure

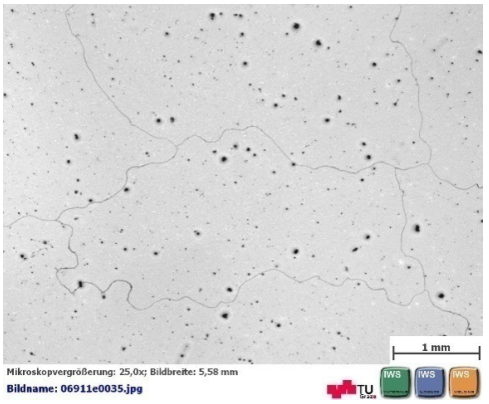

Figure 6: A625 microstructure

	C	Si	Mn	Co	Cr	Mo	V	Ni
Min.	0.12	0.20	0.80	0.90	9.00	1.40	0.18	0.10
Max.	0.14	0.30	1.0	1.10	10.0	1.60	0.22	0.20

Table 1: Major alloying elements COST CB2 steel

	C	Si	Mn	Co	Cr	Fe	Mo	Nb + Ta*
Min	*0.03*	-	-	-	*20.0*	-	*8.00*	*3.15*
Max	0.10	0.50	0.50	1.00	23.0	5.000	10.0	4.20

Table 2: Major alloying elements A625

2.2 Welding

Welding was performed with the *pro-beam* machine EBG 45-150 K14 (EB gun power 45kW, vacuum chamber 1.4m³). All experiments were conducted with an acceleration voltage of 120kV and a circular beam oscillation. No preheating was performed before welding. The welding surfaces for all joints had an average surface finish between Ra=1.6 and 3.2µm. All edges were deburred and the surfaces were cleaned with alcohol.

To find the best welding parameters for these two materials the experimental design and the interpretation of the results was done statistically with the "Design of Experiments" method. Therefore several blind welds (welds in a full metal block) were carried out to evaluate the qualitative and quantitative effects of the welding parameter on the weld. Within these tests, beam current I, welding speed v, focal position fp and the amplitude of the beam figure h were varied.

In the next experimental phase, similar (A625/A625) and dissimilar (A625/CB2) joint samples (see Figure 7) were produced, using different parameter settings. The welding parameters for the dissimilar joint were derived and combined from the results of the blind welding test of the two materials.

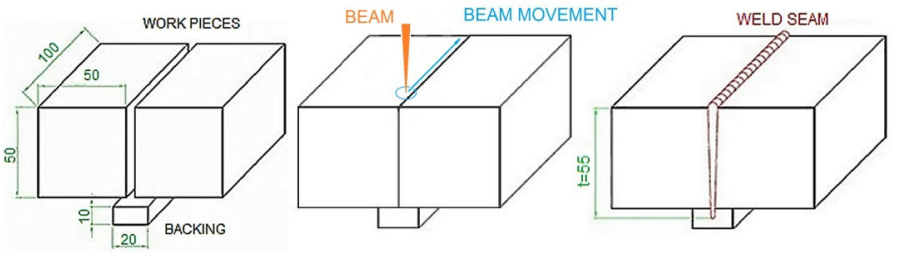

Figure 7: Experiment set up joint samples

Within these experiments the microstructure of the weld, the hardness development across the seam and the mechanical properties of the joint were analysed.

As known from literature, in electron-beam welding very high hardness values, especially for martensitic chromium steels, can be reached [11], [12]. In this study, some of the dissimilar welded mechanical test pieces were subjected to a post weld heat treatment (PWHT) for one hour at 700°C to investigate the influence of this hardness peak and compare it with the test pieces in the as welded (AW) condition.

The microstructural analysis was carried out by means of light optical microscopy after preparing the cross sections with various etchants considering the different materials joined. To investigate the **hardness** distribution several Vickers hardness lines with different loads (HV1 and HV10) were made across the seam and the HAZ in top, middle and root position of the welding. To evaluate the mechanical properties of the seam, tensile test specimens (DIN 50125, mode B) were taken and tested with a constant load rate of 10MPa/s. The Charpy impact energy was measured using samples in VWT (V: Charpy-V notch; W: notch in the fusion zone; T: notch along the thickness, **Error! Reference source not found.**a) and VHT mode (V: Charpy-V notch; H: notch in the heat affected zone; T: notch along the thickness, **Error! Reference source not found.**b) according ÖNORM EN 10045-1.

Furthermore, side bend tests specimens, shown in Figure 8, in accordance to EN ISO 5173 were tested with a maximum bending angle of 180° and a bending rod diameter of 40mm. Due to the different strengths of the materials a support plate had to be used to prevent horizontal shifting of the specimen during the test. The test set up is illustrated in Figure 9.

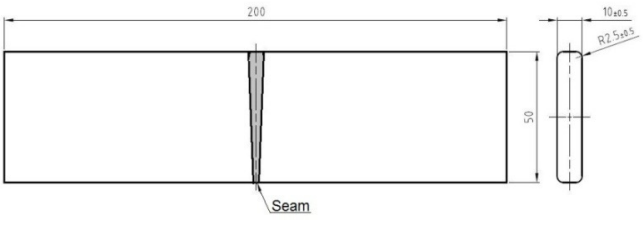

Figure 8: Side bend specimen

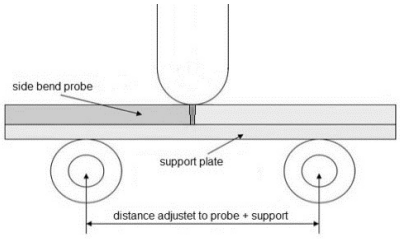

Figure 9: Side bend test set up

3. Results and Discussion

In the blind welding studies proper welding parameters for each material were determined. Obviously both materials show different optimum welding parameters. To achieve a successful joint in dissimilar welding a compromise for the parameters had to be developed.

3.1 Similar Joints (A625/A625)

Microstructure: In none of the performed similar joint welds cavities or cracks were observed when using optimised parameters. Figure 10 shows one representative cross section macro etching of a similar joint (A625/A625). The shape of the seam is steady and the finer grain in the fusion zone is visible with the naked eye. To identify the solidification process, aqua regia was used as etchant. Solidification direction is observed to be perpendicular to the beam describing the direction of the highest temperature gradient. The lines in Figure 11 result from varying solidification speed caused by impurities in alloying elements which induce local undercooled areas. These lines are in this arrangement harmless. A conglomeration of the lines in the seam centre would affect the strength of the joint [18].

Figure 10: Joint welding, similar

Figure 11: Cross section, solidification lines

In Figure 12 and Figure 13 the area next to the fusion zone is displayed. The microstructure of the fusion zone is clearly different compared to the base material; no heat affected zone is visible. However some grain boundaries were found in higher magnification, which grow into the fusion (see Figure 13) which is caused by epitaxy grain growth.

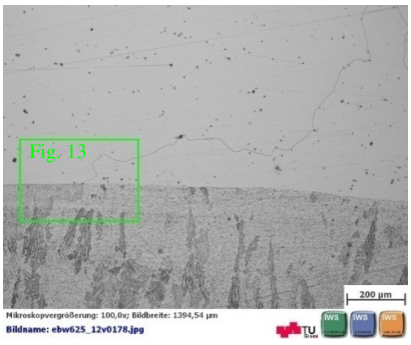

Figure 12: Fusion zone, dendrites

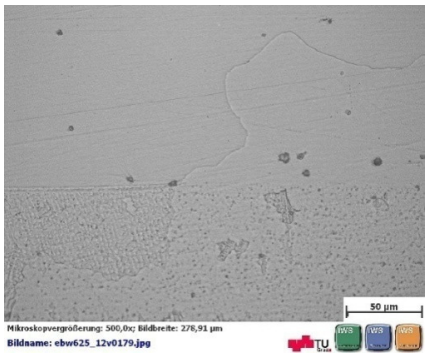

Figure 13: Grain boundary

Hardness: The carried out hardness lines across the seam show a hardness of 160HV10 in the base material. From about 2mm from the fusion zone, the hardness progressively increases to reach a maximum of about 220HV in the centre of the fusion zone which can be explained by the grain refinement.

Tensile test: None of the tested specimen fractured in the fusion zone. The average ultimate tensile strength is 490MPa which is in the range of the tested base material.

Charpy test: Due to the high ductility of A625, just a small percentage of tested pieces fractured and delivered valid results, here the impact energy was always above 215J.

Side Bend test: All welded Nickel based specimens where bent to 180° without any cracks.

3.2 Dissimilar Joints

The materials showed different behaviour with respect to some of the welding parameters; The CB2 needed more welding current to reach a certain depth and a bigger beam figure diameter to produce a stable keyhole. Another aspect for this joint is the magnetic field which is induced during EBW [19]. Especially when welding a magnetic and a non-magnetic material a decent demagnetisation for the CB2 was necessary in order to avoid beam deflection.

Microstructure:

Figure 14 shows one representative cross section of a dissimilar joint. In the light microscope, the microstructure of the fusion zone looks analogous to the similar joints. Dendrites, perpendicular to the beam direction, are visible as well as some solidification lines (see

Figure 15).

Figure 14: Joint welding, dissimilar

Figure 15: Fusion zone, dissimilar

With an EDX line scan, the qualitative composition of the welded materials and the welded zone was estimated. Figure 16 shows the scan across the seam and the evolution of the quantity of the selected elements: Iron (Fe), Nickel (Ni), Chromium (Cr) and Molybdenum (Mo) in the fusion zone.

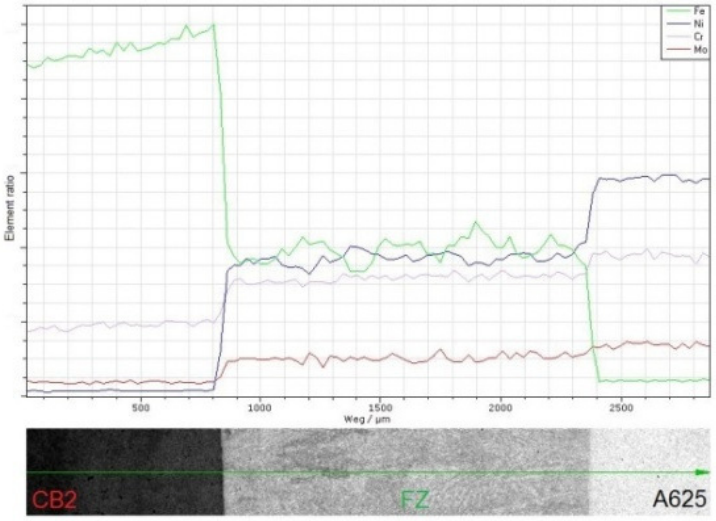

Figure 16: EDX fusion zone; in 25mm depth

It can be seen that there is a quite homogenous distribution of the investigated elements in the fusion zone when the beam is positioned directly on the gap and the oscillation is symmetrical. This indicates a severe convection in the liquid weld pool during the fast welding process. The composition is in between the composition of the two base materials.

The following figures show the heat affected zone neat the CB2 fusion line. Here a very finely striped new formed martensite is visible (Figure 17, arrows). A coarse grained zone ore a zone with tempered martensite was not detectable. This is attributed to the very fast thermal cycle of EBW. Under higher magnification (Figure 18), an approx. 20µm wide area besides the fusion line can be observed where δ-ferrite grains appear (blue areas in Figure 18: Fusion line, CB2/FZ).

Figure 17: Fusion line, CB2/FZ

Figure 18: Fusion line, CB2/FZ

Hardness: In Figure 19, the hardness distribution across a dissimilar joint is shown. In the fusion zone, the hardness increases slightly, although, close to the fusion line on the CB2 side a peak value of 430HV10 is reached which drops down to the hardness of the CB2 base material (240HV10) within 1mm (blue graph Figure 19). The **PWHT** decreased the hardness peak to 265HV10 (red graph in Figure 19), which is below the requested maximum

in the standard (ONORM EN ISO 15614-1 and ISO/TR 15608 material group 9.1). The subsequent investigation shows that during a PWHT at 700°C no visible changes in the microstructure of the A625 are observed. In the HAZ of the CB2, the microstructure now shows tempered martensite.

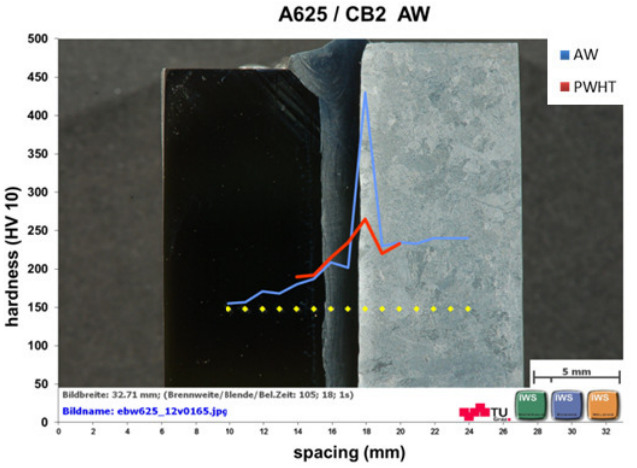

Figure 19: Hardness lines; AW & PWHT

Tensile test: Due to the higher yield strength of the CB2 steel, plastic deformation only occurs on the A625 side. All tensile test samples (PWHT and AW) fractured in the A625 base material. The average tensile strength for the PWHT specimens (551MPa) was slightly higher than for the AW specimens (524MPa).

Charpy test: Due to the different hardness zones in the joint welds there are three points of interest: the HAZ of the A625, the fusion zone (FZ) and the HAZ of the CB2. The following bar chart shows the average impact energies for the different notch positions and conditions (as welded and post weld heat treated). All values are above the impact energy of the CB2 base material.

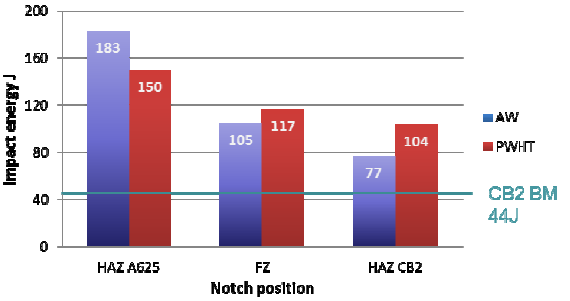

Figure 20: Impact energy [20]

Side bend test: is one of the most crucial tests for a joint. Seven specimens were tested (4x AW, 3 PWHT). All specimens could be bent to 180°, no brittle fracture could be observed despite the high hardness layer next to the fusion line (see Figure 19: Hardness lines; AW & PWHT)! Only one of the PWHT did not meet the requirements according to EN ISO 5173 (> 3mm crack in the FZ). In all test specimens cracks in the CB2 base material were located. The major insight from this test is that the high hardness layer in the CB2 side did not cause a fracture during the bending test.

4. Summary and Conclusion

In this study it was shown that by means of EBW it is possible to weld thick walled components made from a cast 9%Cr steel (CB2) and cast Nickel-based (A625) alloy without pre- and post-heating. After finding appropriate welding parameters the work pieces were welded completely and the joints exhibit good mechanical properties. The investigations of the micro sections and the mechanical test showed that all quality requirements with respect to the microstructure of the weld and its mechanical properties were fulfilled. The very thin high hardness layer, located in the HAZ of the CB2, showed no influence on the mechanical properties. In terms of tensile strength and ductility a PWHT is not necessary.

5. Outlook

Further investigation of the creep behaviour of the welded joint has to be carried out. Particularly, the fine grained fusion zone and the presence of □-ferrite in the HAZ of CB2 are adverse for the creep behaviour. Especially a comparison between a EB welded and MMA welded joint (see [7]) would be interesting. Furthermore the effect of the high hardness layer in the CB2 HAZ on the toughness and fatigue strength should be investigated as well.

References

[1] C. Wiednig, C. Lochbichler, N. Enzinger, C. Beal, and C. Sommtisch, “Dissimilar Electron Beam Welding of Nickel base Alloy 625 and 9% Cr Steel,” in IIW Annual Assembley, 2013.

[2] Max-Planck-Institute für Plasmaphysik, “Annual global primary energy demand without CO2 restriction,” Greifswald, Germany, 2012.

[3] I. Holzer, “Modelling and Simulation of Strengthening in Complex Martensitic 9-12% Cr and a Binary Fe-Cu Alloy,” Graz University of Technology, 2010.

[4] Special Metals Co., “INCONEL alloy 625.” Huntington, US, 2006.

[5] S. K. Rai, A. Kumar, V. Shankar, T. Jayakumar, K. Bhanu Sankara Rao, and B. Raj, “Characterization of microstructures in Inconel 625 using X-ray diffraction peak broadening and lattice parameter measurements,” Scripta Materialia, vol. 51, no. 1, pp. 59–63, Jul. 2004.

[6] ThyssenKrupp, “Nicrofer 6020 hMo - alloy 625,” no. 4118. Werdohl, Germany, 2007.

[7] B. Berger, “Dissimilar Schweißen von Guss-Stücken (Konstruktionsschweißungen) NIBAS 625 mit warmfestem Cr- Stahl COST CB2,” Technische Universität Graz, 2011.

[8] D. Dobeneck v., T. Löwer, and V. Adam, Elektronenstrahlschweißen - Das Verfahren und seine industrielle Anwendung für höchste Produktivität. Burg, Germany: Verlag moderne Industrie, 2001.

[9] W. Behr, “Wettbewerbsfähige Lösungen für die Fügetechnik,” DVS-Aktuell: „Elektronenstrahlschweißen“, 2009.

[10] U. Dilthey, Schweißtechnische Fertigungsverfahren 1 Schweiß- und Schneidtechnologien, 3. Auflage. Berlin- Heidelberg: Springer Verlag, 2006, pp. 157–172.

[11] K. R. Schulze, “Durch dick und dünn - Elektronen strahlschweißen - Verfahren und Technologien,” Schweissen und Schneiden, vol. 63, no. 6, pp. 320–325, 2011.

[12] M. Dobner, “Untersuchungen zum Elektronenstrahlschweißen dickwandiger Bautelle,” Technische Hochschule Aachen, 1996.

[13] Z. Sun and R. Karppi, “The application of electron beam welding for the joining of dissimilar metals: an overview,” Journal of Materials Processing Technology, vol. 59, no. 3, pp. 257–267, May 1996.

[14] K. Woeste, “Elektronenstrahlschweißen metallischer Werkstoffkombinationen,” Reinisch-Westfälische Technische Hochschule Aachen, 2005.

[15] Voestalpine Gießerei Traisen, “Werkstofferprobung GX13CrMoCoVNbNB10-1-1.” Traisen, 2009.

[16] Voestalpine Gießerei Traisen, “Werkstoffdatenblatt NiCr22Mo9Nb; 2.4856.” Traisen, 2007.

[17] G. K. Grossmann and H. Decking, “Verarbeitungshinweise für austenitische Edelstähle und Nickelbasislegierungen.” Essen, Deutschland, 2002.
[18] H. Schultz, Elektronenstrahlschweißen, 2nd ed. Düsseldorf: DVS-Verlag GmbH, 2000.
[19] M. Ziolkowski and H. Brauer, “Modelling of Seebeck effect in electron beam deep welding of dissimilar metals,” COMPEL: The International Journal for Computation and Mathematics in Electrical and Electronic Engineering, vol. 28, no. 1, pp. 140–153, 2009.
[20] D. Dobeneck v., Elektronenstrahlschweißen - Anwendungsbeispiele aus 30 Jahren Lohnschweißpraxis, 2. Auflage. Burg, Germany: pro-beam AG & Co. KGaA, 2007.